

THE DISPERSION OF FIRE SUPPRESSION AGENTS DISCHARGED FROM HIGH PRESSURE VESSELS: ESTABLISHING INITIAL/BOUNDARY CONDITIONS FOR THE FLOW OUTSIDE THE VESSEL

L.Y. Cooper

National Institute of Standards & Technology (NIST), Gaithersburg, USA

ABSTRACT

This is part of a study of dispersion of Halon and Halon-alternative fire extinguishment agents discharged from N_2 -pressurized vessels. As liquid agent exits from the vessel, thermodynamic and fluid-dynamic instabilities lead to flashing and break-up into a two-phase droplet/gaseous jet mixture. This occurs in a transition region relatively close to the vessel exit orifice/nozzle. Downstream, the agent jet is dispersed in the protected space. A model to simulate vessel discharge was developed previously. Using the output of this and thermodynamic and fluid-dynamic considerations of phenomena in the transition region, this paper develops a method for determining time-dependent boundary conditions at an initial section of the jet, downstream of the transition region. These boundary conditions can be used to simulate development and dispersal of the ensuing air/two-phase-agent jet. Applications of the methodology are presented.

INTRODUCTION

The Building and Fire Research Laboratory (BFRL) of the National Institute of Standards and Technology (NIST) is carrying out a Program for the US Air Force to study the dispersion and extinguishment effectiveness of Halon and Halon-alternative fire extinguishment agents discharged from N_2 -pressurized vessels. This is being carried out in support of an effort to advance the technology of fire safety in US Air Force aircraft. One objective of the program is to measure and/or predict the dispersion of a discharging agent throughout a protected space. Time-dependent agent concentrations associated with a particular agent discharge and threat scenario would be used as a basis for estimating extinguishment effectiveness.

This work focuses on one aspect of the problem of predicting agent dispersion by means of mathematical/computer modeling. The strategy involves two basic mathematical model components: 1) a model to simulate the time-dependent discharge of the agent from the high-pressure discharge vessel; and 2) a model to simulate the development and dispersal of the ensuing mixed air/two-phase-agent jet.

A critical element in exercising any component-2 model is a set of initial/boundary conditions for the jet. This must be at a location of the jet axis near the exit section of the discharge vessel. The initial/boundary conditions would be derived from the predictions of the component-1 model. This work develops a method and algorithm to estimate the initial conditions from the predictions of the component-1 model described in [1].

A MODEL OF THE DISCHARGE PROCESS

In response to the above objectives a component-1-type mathematical model of agent discharge was developed in [1]. The model is designed to simulate agent discharge for test or field-deployed system configurations depicted in Figure 1. This involves a cylindrical discharge vessel with a short, circular, exit nozzle/orifice. The vessel is filled with pure agent and pressurized with N_2 to some prescribed value; liquid agent and some dissolved N_2 below and gaseous agent and N_2 above. In the case of a field-deployed system, liquid-agent discharge is initiated with an explosive cap at the exit. A Figure-1 test configuration to simulate field-deployed system discharges under laboratory conditions, is equipped with the indicated high-pressure N_2 holding tank. This is connected to the discharge vessel via an orifice. This system simulates the field-deployed system by using a rupture diaphragm over the exit. (nominal rupture pressure same as the pre-discharge pressure of the field-deployed system) rather than an explosive cap. An experimental run begins with the onset of through-

orifice N_2 flow from the holding tank. The vessel is pressurized to diaphragm rupture followed by vessel discharge to the atmosphere. Note that systems of interest in the present study typically involve initial P_{DV} 's of several tens of atmospheres, where, in the "upside down" Figure-1 configuration and at the time that liquid discharge is being completed, P_{DV} is still large enough to preclude flashing of the liquid in the vessel.

Reference [1] includes a detailed description of the model and results of simulations carried out to establish an experimental design and procedure expected to closely simulate field-deployed system discharges. The model simulates the time-dependent discharge of Figure-1-type systems up to the time that the last of the liquid agent is ejected from the vessel. For a specified set of geometric system parameters, agent material, and initial conditions, key results of a model simulation are $dM_{DV,AL}/dt$ and P_{DV} . This work develops a procedure to use these results with other considerations to estimate initial/boundary conditions for component-2-type model simulations of the development and dispersal of the ensuing mixed air/two-phase-agent jet.

MODELING THE EARLY DEVELOPMENT OF THE JET: FROM THE EXIT SECTION OF THE DISCHARGE VESSEL TO A NEARBY SECTION IN A STATE OF THERMODYNAMIC EQUILIBRIUM AND COMPLETED DROPLET FORMATION

General Considerations. It is assumed that within the discharge vessel and upstream of the exit nozzle/orifice the velocity of the liquid agent is so small that its kinetic energy can be neglected in considerations of its thermodynamic state. Therefore, the thermodynamic state upstream of the nozzle/orifice position can be estimated by P_{DV} and $T_{DV,AL}$. Note that in most applications it is expected that $T_{DV,AL}$ is well approximated by T_{AMB} . A point representing the state of the liquid agent in the vessel is indicated in the sketched pressure-enthalpy (P, h) diagram of Figure 2.

Because of the relatively-short nozzle/orifice design under consideration, the time interval for the liquid to approach it, pass through it, and enter the outside environment is very small. For conditions related to the NIST Program this is of the order of 10^{-3} s. During this time interval the pressure of the traversing liquid is reduced from the high P_{DV} values inside the vessel, of the order of several tens of atmospheres, to pressures of the order of P_{AMB} , one atmosphere.

As discharging liquid enters and traverses the region of the nozzle/orifice, it will enter and move along superheated metastable thermodynamic states. While dependent on its changing thermodynamic state in the vessel

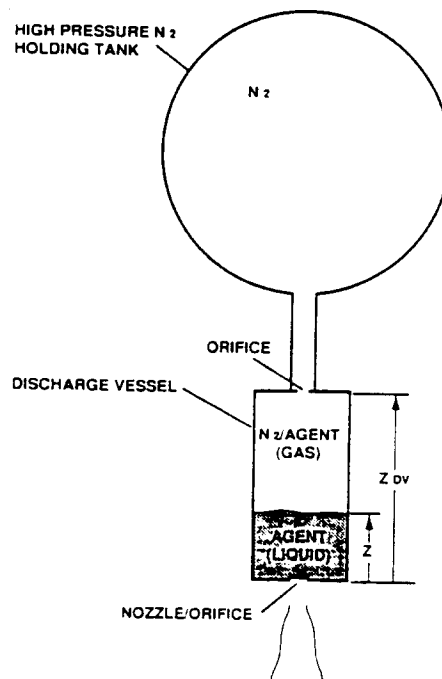


Figure 1. The experimental arrangement.

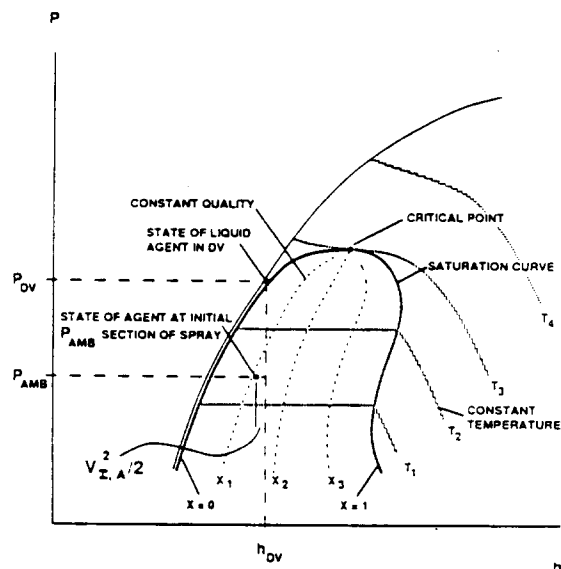


Figure 2. Path in the enthalpy-pressure plane of the thermodynamic state of the initially liquid agent as it flows from inside to outside of the pressure vessel and achieves a stable two-phase state at the initial section.

and on its particular thermodynamic properties, as the agent material penetrates the ambient environment it approaches, and likely achieves P_{AMB} while still in its metastable liquid state. Thus, downstream of a *vena contracta* the liquid agent develops into a near-uniform-radius liquid jet which can be described following traditional incompressible fluid-dynamic considerations. See Figure 3. For the relatively large-vapor-pressure agent materials of interest here, a combination of fluid-dynamic and thermodynamic instabilities will then lead to breakup into small droplets and flashing (i.e., rapid evaporation to a two-phase equilibrium thermodynamic state) of the metastable liquid jet [2].

The metastable liquid is expected to move through thermodynamic states on near-isentropic paths. However, as discussed in [1], for a given agent and initial state conditions it is possible that the pressure along such a path will not reach P_{AMB} prior to an intersection with the agent's spinoidal curve. Moreover, if such an intersection does occur, then at that instant spontaneous nucleation in the liquid is to be expected [3, 4]. It is conjectured that this would lead to near-explosive breakup and flashing of the jet, all of this being initiated within a jet penetration depth (into the outside environment) of the order of a single nozzle/orifice diameter.

Whatever the thermodynamic-state path of the discharging metastable liquid, it is reasonable to assume that a relatively short distance downstream of the nozzle/orifice a thermodynamic equilibrium state and an end to the droplet-formation phenomenon will be achieved. It is also reasonable to assume that, as the agent flows further downstream, developing as a mixed, two-phase, agent/air jet, thermodynamic equilibrium will be maintained, and droplet collision and agglomeration will not play an important role in jet dynamics.

The Initial Section of the Jet. The position along the jet axis where both approximate thermodynamic equilibrium and completion of droplet formation is first achieved will be denoted here as the *initial* position of the jet. Associated with this position is the plane section normal to the jet axis, called the *initial* section of the jet. Similarly, the thermodynamic state and properties of the jet at the *initial* position will be denoted as its *initial* state and *initial* properties. The region of the flow between the nozzle/orifice discharge section and the *initial* section will be referred to as the transition region of the jet.

A detailed description of the *initial* state and properties of the jet would be extremely complicated. This would include the variation across the *initial* section of air/gaseous-agent concentrations, temperature, and velocity, and of the size, velocity, and temperature distributions of the liquid agent droplets. Note also that in the present application all of these variables of the jet at the *initial* section would be time-dependent. In general, a detailed description of the jet at the *initial* section, whether determined by theoretical or experimental means, is either impractical or beyond the current state of technology.

Although it is not possible to provide a detailed description of the *initial* state of the jet, an achievable approximate description, suitable for use in a component-2-type model, should yield good approximations of the dispersing-agent-flow-field problem. It is the purpose of this work to provide such a description.

Assumptions of Phenomena in the Transition Region: From Nozzle/Orifice to Initial Section. The dynamic processes that initiate breakup and flashing of the metastable liquid jet and bring it to its *initial* state are not completely understood. At one extreme, it is possible that the above-mentioned instabilities lead to violent

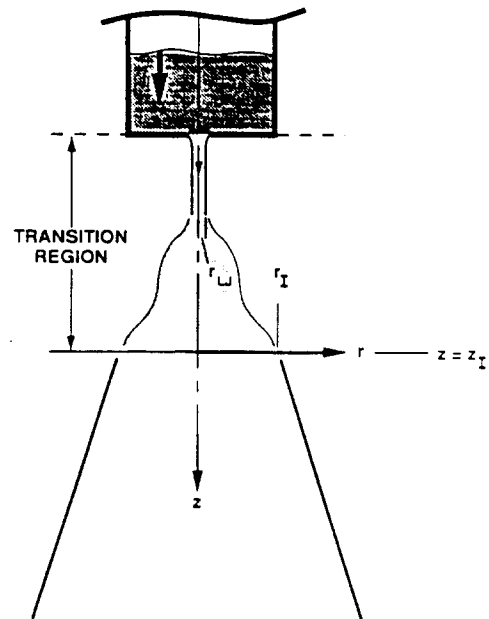


Figure 3. Sketch of the discharging agent, the transition region, and the initial section, $z = z_I$.

breakup and flashing of the liquid jet immediately upon leaving the exit nozzle/orifice. Such behavior was observed, for example, in some experiments of [5]. Also, toward the completion of the liquid discharge, this was also observed in recent experiments at NIST [6].

The metastable state can also persist even as the liquid jet penetrates relatively deeply into the ambient environment. For example, Reference [5] describes a liquid water jet of diameter $D = 7.6(10^{-4})\text{m}$, initially at $9.03 \times 10^5 \text{Pa}$ and 415K , which penetrated up to 0.0254m , corresponding to $L/D = 32$, before initiation of violent breakup/flashing. Observed in the recent NIST experiments [6] was a liquid Freon 22 jet, $D = 0.02\text{m}$, initially at $41.37 \times 10^5 \text{Pa}$ and 294K , which penetrated a distance of approximately 0.3m , corresponding to $L/D = 15$, before initiation of violent breakup/flashing. In this regard it is of interest to note that in the literature of the discharge of flashing liquids from high pressure vessels there is a degree of conventional wisdom that analyses of the two-phase flow phenomena, based on thermodynamic equilibrium states, tend to yield good results when the nozzle/piping from the inside to the outside of a discharge vessel is at least 0.1m [7].

The initial section will be some incremental distance downstream of the penetration distance of the metastable liquid jet. The studies of [5] and the recent experiments at NIST [6] suggest that this distance will typically not exceed the order of the penetration distance itself. Whatever the distance, it is assumed here that the total length of the transition region is small enough, compared to the characteristic length of the overall agent dispersal problem of interest, that the processes within the transition region can be treated as quasi-steady.

In the transition region it is assumed that momentum transfer and work or heat transfer interactions between the agent jet and the ambient environment are negligible. Thus, consistent with the analysis of [8] for steady, two-phase, air/evaporating-liquid jets, it is assumed that the jet at the initial section can be approximated as consisting only of a two-phase mixture of agent, with no entrained air. Finally, in the transition section it is assumed that increases in the energy of the liquid due to mechanical work by surface tension forces to form the initial-section droplets are negligible compared to the energy transfers of the phase-change processes.

The Initial State - A Summary of Assumptions and Approximations and Their Implications. Regarding an estimate of the initial state, the assumptions of the previous paragraph, some additional approximations and assumptions, and their implications are now summarized.

At the initial section, $r \leq r_I$ consists of a pure mixture of saturated-agent vapor and liquid (droplets) in thermodynamic equilibrium, where

$$P_I = P_{\text{AMB}}; \quad r \leq r_I; \quad T_I = T_{\text{SAT}} = T_{\text{SAT}}(P_{\text{AMB}}), \quad r \leq r_I; \quad T_{\text{SAT}} = T_{\text{SAT}}(P), \quad P \leq P_{\text{CR}} \quad (1)$$

T_{SAT} is a specified function of P , where P can not exceed P_{CR} . The liquid-agent component of the jet consists of droplets of uniform-radius and these are uniformly dispersed over the region $r \leq r_I$. There is no agent in $r > r_I$. The agent droplets and gas have the same uniform axial jet velocity, $V_{I,A}$.

$$V_I = V_{I,A}; \quad r \leq r_I \quad (2)$$

The region $r > r_I$ consists of a uniform ambient-temperature/pressure environment of quiescent air. There is no air in $r \leq r_I$.

$$P_I = P_{\text{AMB}}; \quad T_I = T_{\text{AMB}}; \quad V_I = V_{I,AIR} = 0; \quad r > r_I \quad (3)$$

Conservation of mass leads to

$$\pi r_I^2 V_{I,A} \rho_{I,A} = dM_{DV,AL}/dt; \quad \rho_{I,A} = 1/[x_I/\rho_{I,AG} + (1 - x_I)/\rho_{I,AL}] \quad (4)$$

The right side of the first of Eqs. (4), determined previously from, e.g., the discharge model of [1], is assumed to be specified. Conservation of energy and Eq. (4) lead to

$$h_{DV,AL} = h_{I,AL} + x_I h_{ALG}(T_{\text{SAT}}) + V_{I,A}^2/2; \quad h_{ALG}(T_{\text{SAT}}) = h_{I,AG} - h_{I,AL} \quad (5)$$

A point representing the state of the agent at the initial section is presented in the (P, h) diagram of Figure 2. Consistent with Eqs. (5), this reflects the fact that some of the original enthalpy of the material in its high pressure "rest" state was exchanged for its now-significant kinetic energy. The sketch of the transition region and of the initial properties as presented in Figure 3 is consistent with the all the above assumptions/approximations.

It is assumed that the droplet diameter is specified. Based on [5] it is expected that this will be in the range 10-100 μ m. Photographic data during future NIST experiments should provide sharper estimates of this parameter. Also, the sensitivity of the downstream agent concentrations to variations of this parameter should be evaluated with component-2 model simulations.

Regarding the initial jet radius, it is assumed that r_I is specified. Based on photographic data in [5] and on photographic data already acquired during NIST experiments, r_I/r_{LJ} seems to be of the order of 10 - 20. Thus, in (what is reasonable to construe visually in high speed photographs as) a region of breakup and flashing of the liquid jet to an initial equilibrium state, the radius of the jet increases by a factor of 10 - 20. Again, the sensitivity of the downstream agent concentrations to variations of this ratio should be evaluated with component-2 model simulations. One would hope that such sensitivity is not great.

Consistent with the above, the specified parameters of the initial state are P_I , from the first of Eqs. (1), $r_{I,D}$, and r_I/r_{LJ} . Also, for a particular agent of interest, T_I is specified by the second and third of Eqs. (1). Required to complete the description of the initial state are $\rho_{I,AL}$, $V_{I,A}$, and x_I .

Completing the Description of the Initial State. For problems of interest here, agent liquid temperatures are expected to be small enough compared to T_{CR} and vary in a small enough range to permit accurate modeling of the liquid as having constant properties. These are taken to be

$$T_{AL} = (T_{SAT} + T_{DV,AL})/2; \quad \rho_{AL} = \rho_{AL}(T_{AL}); \quad C_{AL} = C_{AL}(T_{AL}) \quad (6)$$

Also, the agent gas is modeled as a perfect gas. Finally, Bernoulli's equation is used to determine the rate of outflow of (liquid) agent, where it is assumed that the liquid jet achieves P_{AMB} prior to breakup/flashing.

ALGORITHM FOR DETERMINING THE INITIAL STATE

The details of invoking the above methodology are presented in [9]. These lead to the following algorithm for determining the initial state:

1. Specify agent and its thermodynamic properties, including $T_{SAT}(P)$, $h_{ALG}(T)$, $\rho_{AL}(T)$, and $C_{AL}(T)$.
2. Specify r_I/r_{LJ} (expected range 10 - 20).
3. Specify P_{AMB} , T_{AMB} , and $T_{DV,AL}$. (In most cases expect to specify $T_{DV,AL} = T_{AMB}$.)
4. Specify $T_I = T_{AMB}$ for $r > r_I$. Compute $T_{SAT}(P_{AMB})$ and then specify $T_I = T_{SAT}$ for $0 \leq r \leq r_I$.
5. Compute $h_{ALG}(T_{SAT})$.
6. Compute T_{AL} , ρ_{AL} , and C_{AL} according to Eqs. (6).
7. Compute $\rho_{I,AG}$ and then ε according to

$$\rho_{I,AG} = P_I/(R_{AG}T_I) = P_{AMB}/(R_{AG}T_{SAT}); \quad \varepsilon = \rho_{I,AG}/\rho_{AL} \quad (7)$$

8. Use a component-1 model, e.g., that of [1], to find $P_{DV}(t)$ for the Figure-1-configuration of interest.
9. For a particular value of P_{DV} compute, sequentially, λ_1 , λ_2 , X , x_I , and $V_{I,A}$ from

$$\begin{aligned} \lambda_1 &= \rho_{AL}C_{AL}(T_{DV,AL} - T_{SAT})/(P_{DV} - P_{AMB}); \\ \lambda_2 &= [\varepsilon/(1 - \varepsilon)]\rho_{AL}h_{ALG}(T_{SAT})/[(P_{DV} - P_{AMB})(r_{LJ}/r_I)^2]; \\ X &= -(\lambda_2/2) + [(\lambda_2/2)^2 + \lambda_1 + 1]^{1/2} \\ x_I &= X\varepsilon/[(1 - \varepsilon)(r_{LJ}/r_I)^2]; \quad V_{I,A} = 2X[(P_{DV} - P_{AMB})/\rho_{AL}]^{1/2} \end{aligned} \quad (8)$$

EXAMPLE APPLICATION OF THE ALGORITHM

Conditions for Example Discharges and Temperature-Dependent Agent Property Functions. The algorithm

was applied in four example discharge simulations. These involve the agents Freon 22 (CHClF_2) and Halon 1301 (CBrF_3) and two different r_I values corresponding to $r_I = 10r_{LJ}$ and $20r_{LJ}$. The examples consider time-dependent agent discharges from a Figure-1 configuration with no holding tank. The geometric parameters, $C_D = (r_{LJ}/r_N)^2$, and initial conditions assumed in the simulated discharges are

$$V_{DV} = 0.500 \times 10^{-3} \text{ m}^3; A_{DV} = 0.1963 \times 10^{-2} \text{ m}^2; r_N = 0.9525 \times 10^{-2} \text{ m}; C_D = 0.6; T_{DV,AL} = 294 \text{ K};$$

$$\text{at } t = 0: V_{DV,AL} = 0.250 \times 10^{-3} \text{ m}^3; T_{DV} = 294 \text{ K}; P_{DV} = 41.36 \times 10^5 \text{ Pa}$$

These are the same parameters used in the example calculations of [1]. During the discharge, the time-dependent value of P_{DV} was computed using the component-1-type model of [1]. The property functions for Freon 22 (CHClF_2) and Halon 1301 (CBrF_3), were taken from [10].

Results of the Example Calculations. Results of the example calculations, including ζ , are tabulated in [9].

$$\zeta = M_{DV,AL}/M_{DV,AL}(t=0) = Z/Z(t=0) \quad (9)$$

Results for the discharge of Freon 22 ($r_I = 10r_{LJ} = 0.07378 \text{ m}$), where $M_{DV,AL}(t=0) = 0.33 \text{ kg}$, are plotted in Figures 3a-d. Included are P_{DV} (Figure 4a), $V_{I,A}$ (Figure 4b), ζ and x_I (Figure 4c), and $dM_{I,AL}/dt$ and $dM_{I,AG}/dt$ (Figure 4d).

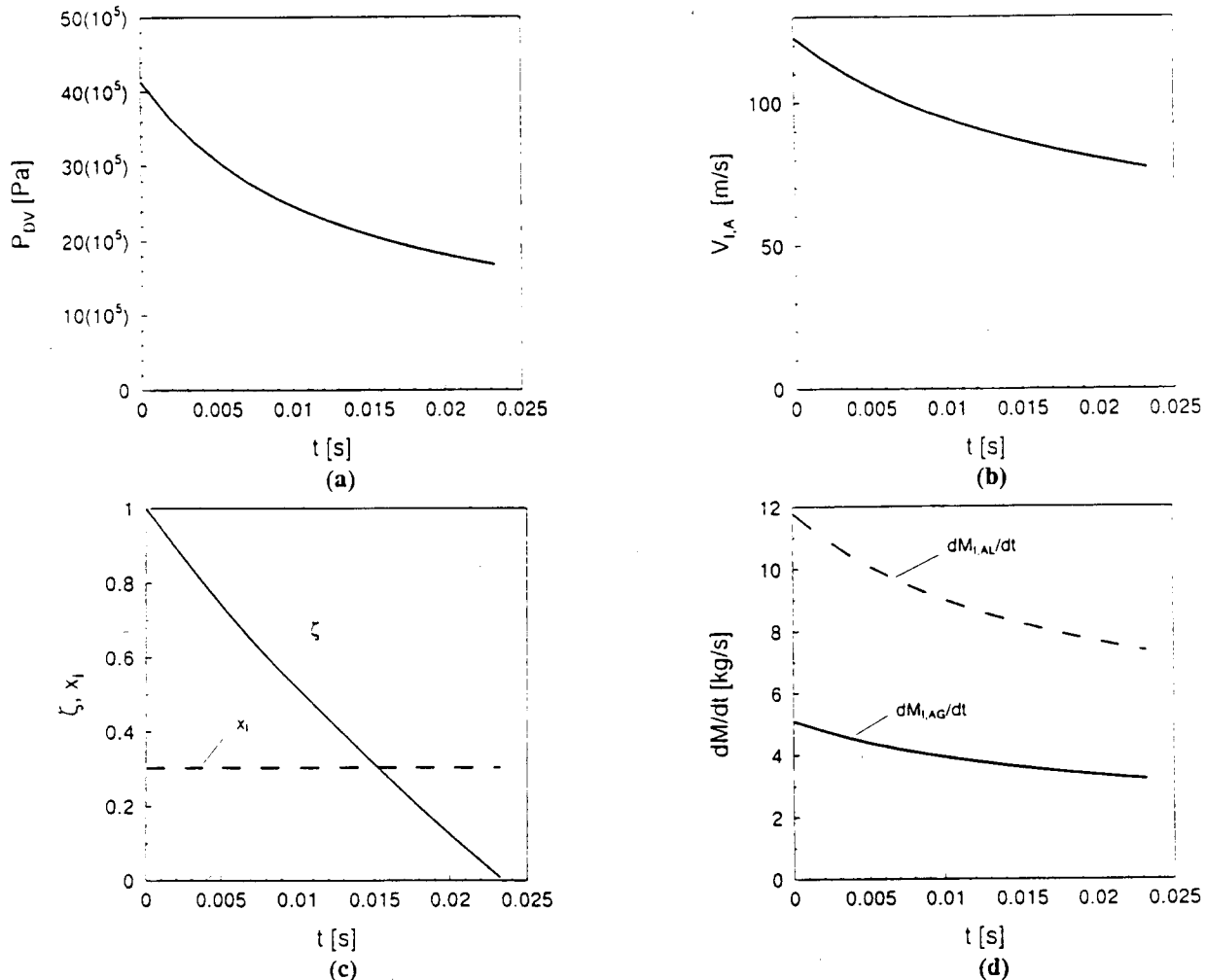


Figure 4. Calculated vessel discharge of Freon 22 - plots of results for time dependence of: (a) P_{DV} ; (b) $V_{I,A}$; (c) ζ and x_I ; and (d) $dM_{I,AL}/dt$ and $dM_{I,AG}/dt$.

A study of the results leads to the following observations:

1. For both Freon 22 and Halon 1301, the times to complete the discharge of liquid agent from the pressure vessel are almost identical at 0.024 ± 0.001 s.
2. At the initial section, the quality of the two-phase agent flow, x_1 , is significantly different for the two agents considered, but for a given agent x_1 is relatively independent of t and r_1 , for the two initial-section radii values considered ($r_1 = 0.07378$ m and 0.1476 m). Thus, for the cases considered, $x_1 = 0.31 \pm 0.01$ for Freon 22 and $x_1 = 0.54 \pm 0.02$ for Halon 1301.
3. At the initial section, for a given agent, and for the two initial-section radii values considered, the mass flow rates of liquid or gaseous agent are almost identical at any particular time during the discharge. [For example: for Freon 22, approximately half-way through the discharge at $t = 0.01252$ s, values of $dM_{I,AL}/dt$ for $r_1 = 0.07378$ m and $r_1 = 0.1476$ m are 8.59 kg/s and 8.49 kg/s, respectively; and for Halon 1301, approximately half-way through the discharge at $t = 0.01222$ s, values for $dM_{I,AL}/dt$ for $r_1 = 0.07378$ m and $r_1 = 0.1476$ m are 6.95 kg/s and 8.59 kg/s, respectively.] However, over the course of the discharge, these mass flow rates are reduced to approximately two thirds of their initial value. [For example: for Freon 22 and $r_1 = 0.07378$, the values of $dM_{I,AL}/dt$ at $t = 0$ and $t = 0.2326$ s (near the end of the liquid discharge) are 11.78 kg/s and 7.34 kg/s, respectively (Figure 4); and for Halon 1301, and $r_1 = 0.07378$, the values of $dM_{I,AL}/dt$ at $t = 0$ and $t = 0.2443$ s (near the end of the liquid discharge) are 9.26 kg/s and 5.88 kg/s, respectively.]

ACKNOWLEDGEMENT

The author acknowledges the U.S. Air Force, U.S. Navy, U.S. Army, and U.S. Federal Aviation Administration for funding the Agent Screening for Halon 1301 Aviation Replacement project under the direction of Mr. Michael Bennett at the Wright Patterson Air Force Base.

NOMENCLATURE

C_{AL}	specific heat of liquid agent
C_D	orifice coefficient
D	diameter of a liquid jet
h	specific enthalpy
h_{ALG}	agent heat of vaporization
$h_{DV,AL}$	h of agent liquid in discharge vessel
$h_{I,AG}; h_{I,AL}$	h at <u>initial</u> section of: agent gas; agent liquid
L	length of liquid jet
$dM_{I,AG}/dt;$ $dM_{I,AL}/dt$	mass flow rate at <u>initial</u> section of: agent gas; agent liquid
$M_{DV,AL}$	mass of liquid agent in discharge vessel
P	pressure
$P_{AMB}; P_{DV}; P_I$	P : of ambient; in discharge vessel; at <u>initial</u> section
P_{CR}	critical pressure of agent
R_{AG}	gas constant for agent gas
r	radius
$r_I; r_{LJ}; r_N$	r of: jet at <u>initial</u> section; liquid jet; nozzle/orifice
T	absolute temperature
$T_{AL}; T_{AMB};$ $T_{DV}; T_{DV,AL};$ $T_I; T_{SAT}$	T : of agent liquid; of ambient; of agent gas in discharge vessel; of agent liquid in discharge vessel; at <u>initial</u> section; of saturated agent
V_{DV}	volume of discharge vessel
$V_{DV,AL}$	volume of liquid agent in discharge vessel
V_I	velocity at the <u>initial</u> section
$V_{I,A}; V_{I,AIR}$	V_I of: agent; air
X	Eq. (8)
x_1	quality of two-phase agent flow at <u>initial</u> section
Z	elevation above exit nozzle/orifice of liquid/gas agent interface in discharge vessel
ϵ	Eqs. (7)
λ_1, λ_2	Eqs. (8)

$\rho_{I,A}$	average density of the agent jet at the <u>initial</u> section
$\rho_{A,L}$	density of agent liquid
$\rho_{I,AG}; \rho_{I,AL}$	density at <u>initial</u> section of: agent liquid; agent gas
ζ	dimensionless elevation of the liquid/gas interface, Eq. (9)

REFERENCES

1. L.Y. Cooper, Discharge of Fire Suppression Agents from a Pressurized Vessel: A Mathematical Model and Its Application to Experimental Design, National Institute of Standards and Technology, NISTIR 5181, Gaithersburg MD, 1993; also Proceedings of Halon Alternatives Technical Working Conference 1993, University of New Mexico, New Mexico Engineering Research Center for Global Environmental Technologies, Albuquerque NM, pp. 530-549, 1993.
2. J.H. Leinhard and J.B. Day, The Breakup of Superheated Liquid Jets, Journal of Basic Engineering, pp. 515-522, September 1970.
3. R.C. Reid, Superheated Liquids - A Laboratory Curiosity and, Possibly, an Industrial Curse, Chemical Engineering Education, pp. 60-87, Spring 1978.
4. M. Modell and R.C. Reid, Thermodynamics and Its Applications, Prentice Hall, 2nd Edition, 1983.
5. R. Brown and J.L. York, Spray Formed by Flashing Liquid Jets, AIChE Journal, Vol. 8, No. 2, pp. 149-153, May 1962.
6. C. Yang, private communication, National Institute of Standards and Technology, Gaithersburg MD, 1992.
7. J.C. Leung and F.N. Nazario, Two-Phase Flashing Flow Methods and Comparisons, Journal Loss Prevention Process Industry, Vol. 3, pp. 253-260, April 1990.
8. M. Epstein et al, One-Dimensional Modeling of Two-Phase Jet Expansion and Impingement, Thermal-Hydraulics of Nuclear Reactors, Vol. II, 2nd International Topical Meeting on Nuclear Reactor Thermal Hydraulics, Santa Barbara California Jan. 11-14, 1983.
9. L.Y. Cooper, The Dispersion of Fire Suppression Agents Discharged from High Pressure Vessels: Establishing Initial/Boundary Conditions for the Flow Outside the Vessel, National Institute of Standards and Technology, NISTIR 5219, Gaithersburg MD, 1993.
10. T.E. Daubert and R.P. Danner, Physical and Thermodynamic Properties of Pure Chemicals, Hemisphere, 1992.